Solvent relaxation and electron back transfer following photoinduced electron transfer in an ensemble of randomly distributed donors and acceptors

Y. Lin,[a] R. C. Dorfman, and M. D. Fayer
Department of Chemistry, Stanford University, Stanford, California 94305

(Received 17 November 1989; accepted 1 May 1990)

The role of solvent relaxation in electron back transfer following electron transfer from an optically excited donor to randomly distributed acceptors is treated theoretically. The solvent dynamics are included by using a time dependent electron back transfer rate function, $K_{\text{eff}}(R,t)$. The solvent relaxation is parameterized by τ_r, the relaxation time, D, the solvent energy diffusion constant, and Δq, the potential barrier height difference between the nonequilibrium solvent state formed upon ion creation and the relaxed solvent state. The expression for the ensemble averaged donor cation state population probability, $\langle P_{ct}(t)\rangle$, as a function of these solvent relaxation parameters is derived. Numerical calculations are presented. Relationships among $\langle P_{ct}(t)\rangle$, the intermolecular interaction parameters, and solvent relaxation parameters provide detailed insights into the distance and time dependence of the flow of electron probability in an ensemble of donors and acceptors. The theoretical expressions can be used to calculate experimental observables such as the transient grating signal.

I. INTRODUCTION

Photoinduced electron transfer is one of the fundamental processes in the realm of chemical reactions. Following the transfer of an electron from a donor to an acceptor, the resulting radical ions are highly reactive species which can go on to do useful chemistry. Electron back transfer, however, quenches the ions and prevents further chemistry from occuring. The initial steps of photosynthesis involve excitation of a donor followed by electron transfer. Electron back transfer to the primary donor turns off the photosynthetic process. In photosynthesis, a specialized spatial array of consecutive acceptors overcomes the back transfer problem and is responsible for the efficiency of photosynthesis.[1-4] In systems of randomly distributed donors and acceptors (liquid or solid solutions) back transfer can be very rapid. In liquid solutions, back transfer competes with diffusional separation of the photoinduced ions and limits chemical yields. Therefore, understanding phenomena which influence back transfer is not only an important basic problem, it is a problem of considerable practical significance.

The results that have come out of many experimental investigations on a wide range of systems and conditions have demonstrated that there is more to photoinduced electron transfer than "particle hopping"[5-13] between molecules in intimate contact. It has been shown that electron transfer depends not only on the distance between donors and acceptors[8,12,14-17] but also on factors such as exothermicity,[18-20] reorganization energy,[2,5,21] temperature,[6,7,22] solvent polarity,[23] molecular spacer (for intramolecular electron transfer),[5,14] and electric field.[3,24] This has motivated theoretical investigations into the dependence of the electron transfer rate on each of these factors.[14,18,22,25-28]

When an ion is suddenly created in a polar solvent, the solvent dipoles begin to move under the influence of the static electric field produced by the ion. The dipoles will align to counter the ion's electric field. The interaction between the ion and the moving dipoles will induce shifts in the energy levels of the ion. As time progresses, a new solvent structure will form about the abruptly created ion. These events are known as solvent relaxation.

In a photoinduced electron transfer process, involving electron transfer from an optically excited donor to an acceptor, the situation is somewhat different for that described immediately above. Following optical excitation there is, in general, a potential barrier separating the neutral donor–acceptor pair from the ions.[1,2] This barrier must be surmounted as part of the electron transfer process. Thermal activation of the neutrals brings the system to the transition state.[1,2,21] Qualitatively, the activation process can be separated into two sets of coordinates which must be perturbed from their equilibrium values to reach the transition state and for electron transfer to occur. These are internal molecular coordinates, labeled by the state energy χ, and external solvent coordinates, labeled by the state energy q. Initially the excited donor and acceptor are in their neutral equilibrium configurations, χ_n, q_n. Thermal activation takes them to the transition state for electron transfer, χ_0, q_0. Extremely rapid relaxation of the internal coordinates, on a time scale of molecular vibrations (10–100 fs), traps the system in the ionic state. Relaxation back to neutrals can occur (barrier recrossing) prior to relaxation of the internal coordinates.[1,2,21] This does not appear as an electron transfer event, and in part determines the forward electron transfer rate parameters. The solvent relaxation generally occurs on a slower time scale, several hundreds of femtoseconds to

[a] Permanent address: Argonne National Laboratory, Argonne, Illinois 60439.

 0021-9606/90/173550-12$03.00

many picoseconds.[30–32] The solvent relaxation process starts from solvent state q_0 and evolves towards the solvent structure totally relaxed about the ions, described by state q_∞. Therefore, the solvent relaxation starts from state q_0 which is intermediate between q_n and q_∞. This is in contrast to an ion which is abruptly created by capturing an electron in a sample being bombarded by electrons. It is also different from solvent relaxation about a molecule which has suddenly undergone a major change in dipole moment upon optical excitation. In these situations, solvent relaxation begins from the equilibrium solvent structure, not from a transition state, q_0. Another feature of solvent relaxation following optically induced electron transfer is that the internal state, following relaxation from χ_0 to χ_∞, may evolve somewhat in response to the solvent relaxation. In what follows any such evolution of χ_∞ will not be distinguished from the solvent relaxation itself.

The role of solvent relaxation can be considerable in modifying processes in and around ions or excited molecules with large permanent dipole moments. Solvent relaxation has become the focus of a number of experimental and theoretical investigations.[9–11,26,27,29–35] Recently, there have been several excellent reviews of this area.[29–32] Time dependent spectral and fluorescence shifts[30,32] and more recently electron transfer have been probes for solvent relaxation processes.[34,35] Yet due to the complexity of the problem of electron transfer with eventual geminate recombination (electron back transfer between the initially created ion pair) in an ensemble of randomly distributed donors and acceptors, a theory relating dynamical properties of the solvent and the electron transfer system to time dependent experimental observables has been lacking.

The problem of forward transfer without solvent relaxation has been solved by Inokuti and Hirayama.[36] In a previous paper,[37] the problem of electron transfer with eventual geminate recombination in an ensemble of randomly distributed donors and acceptors was analyzed. In the paper, the many particle problem was reduced to a two particle problem. The standard method for attacking such a problem is to solve the coupled differential equations governing the various state probabilities, ensemble average over all possible configurations of acceptors, and then pass to the thermodynamic limit. This formal solution leads to multidimensional integrals of dimension n, where n is the number of acceptors. The problem was reduced to a two particle calculation[37] by first averaging over $n-1$ acceptors, then solving the differential equations. The probabilities were averaged over the final spatial coordinate and then passed to the thermodynamic limit. The method provided an exact solution. This not only made the study of the back transfer tractable but also reduced the mathematical complexity to the point that it is possible to include solvent relaxation and diffusion[38] in the calculations. The theory used an electron transfer rate that depended only on the donor–acceptor separation, with excluded volume properly taken into account. Ensemble averaged state probabilities were derived and subsequently used to calculate experimental observables (such as fluorescence and transient grating). Other quantities such as the average ion separation and existence time were also calculated. Calculations were compared to experiments which had a 100 ps time resolution and excellent agreement was obtained.[39]

Solvent relaxation can have a profound effect on the rate of electron back transfer. In the absence of solvent relaxation, for fixed molecular positions, the back transfer rates are time independent. Solvent relaxation will make the back transfer rates time dependent. In general solvent relaxation is much faster than the time scale for significant molecular diffusion in liquids. Therefore, it is sufficient to consider the influence of solvent relaxation on back transfer for fixed donor and acceptor positions. When the ion pair is created, the initial solvent configuration is intermediate between that of the solvent surrounding the neutral molecules at equilibrium and the solvent surrounding the ions at equilibrium. As time evolves, solvent relaxation moves the system away from this initial state. As the solvent relaxes about the ions an increasingly large solvent structure change is required to return the system to neutral molecules (geminate recombination). Thus, solvent relaxation slows the rate of back transfer. Back transfer at short time can be substantially faster than back transfer once solvent relaxation is complete. Therefore, it is important to include solvent relaxation effects in the description of back transfer, and a study of the time dependent rate of back transfer on a picosecond and subpicosecond time scale can be used as a probe of solvent relaxation.

In liquids, which are of particular interest, solvent relaxation times are typically shorter than 100 ps.[14,28,40–42] Relaxation also occurs in solids. In crystals the dressing of an exiton or a polaron by lattice phonons (relaxation of the lattice around an excitation or an electron) occurs on a picosecond time scale. In solid solutions of donor and acceptor molecules in room temperature glasses such as polymeric glasses or sucrose octaacetate which has recently been used in electron transfer experiments,[39] there is a wide distribution of time scales. The distribution can be roughly devided into a short component and a long component. Consider a polymer. Pendant groups will move rapidly in their free volume. Flexing, bending, and rotations of polar groups will be responsible for solvent relaxation in a solid solution on a time scale of less than 100 ps. In addition there can be motions in glasses on very long time scales, milliseconds and longer, from backbone motions of polymer chains, including crankshaft motions and translational diffusion. The latter can occur over hours or days. In small molecule glasses which are generally formed at low temperatures, structural changes by diffusion will also be very slow. For the subject under consideration, the influence of solvent relaxation on electron back transfer dynamics, only the fast component of the relaxation in glasses is important. The slow component occurs on a time scale that is taken to be static. Therefore, for liquids, crystals, and glasses, the relevant time scale for solvent relaxation is taken to be faster than 100 ps.

It is the aim of this paper to include solvent relaxation in the theory previously developed for forward and back electron transfer. We use a simple, yet reasonable, model for solvent relaxation, but any model for the solvent dynamics that gives an electron transfer rate which evolves in time can be used. The essence of the problem is to include the time

dependent back transfer rate into the averages over the distance dependence of the forward and back transfer rates.

In the following, a distribution function for the time dependent ion probability in various solvent states is derived. Next a time and distance dependent back electron transfer rate is obtained. The rate has a distance dependent part that falls off exponentially with distance and a part that depends on the amount of solvation, which is similar to the Marcus' theory exponentially activated rate.[2,21] Finally, the total ion probability function is derived and ensemble averaged.

Using these results, the ion probability as a function of time and distance was calculated for a variety of solvent relaxation times and solvation energies. It will be shown that the time and spatial distributions of ions change as a function of the solvent parameters. The transient grating observable will also be derived.

II. THEORETICAL DEVELOPMENT

In this section the donor cation state population probability, $\langle P_{ct}(t)\rangle$, will be derived. In the derivation the effect of solvent molecule reorganization under the electric field of the radical ions is included. In the model, low concentration donors and high concentration acceptors are randomly distributed and kept in fixed positions. The concentration of donor molecules is low enough that donor–donor electronic excitation transfer is negligible. Because the thermodynamic lowest energy state of the system is a neutral donor and neutral acceptor and spatial diffusion of the molecules does not occur on the time scale of interest, back transfer is geminate as in a solid solution. Because of the systems energetics, the anionic acceptor will not transfer the electron to a neutral acceptor, but only back to the cationic donor. This is the down hill pathway.

An illustration of the electron transfer processes including the solvent states is shown in Fig. 1. At time $t = 0$ an ensemble of dilute donors is optically excited. In the absence of acceptors, the probability of finding the donor still excited at time t, $\langle P_{ex}(t)\rangle$, decays exponentially with the excited state life time τ, where $\langle P_{ex}(t)\rangle = \exp(-t/\tau)$. When acceptors are present the probability decreases more rapidly due to the addition of the electron transfer pathway for quenching the electronic excited state.

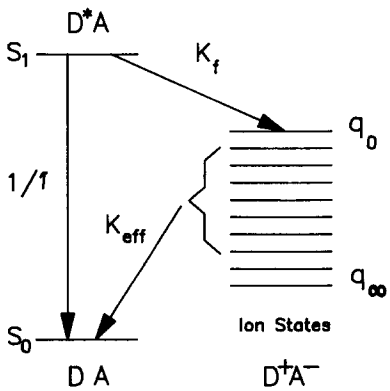

FIG. 1. Energy level diagram. DA, D^*A, and D^+A^- are the ground state neutral donor and acceptor, excited donor and ground state neutral acceptor, ground state cation and anion, respectively. The diagram shows only one of the n acceptors. Forward electron transfer from the excited donor state to the acceptor is into the q_0 solvent state and back transfer is from any of the ion states with solvent configuration designated by q. q_∞ represents the solvent state after solvent relaxation about the ions is complete.

The electron transfer reaction occurs in the following stages: After excitation a fraction of the donor–acceptor systems is thermally promoted to their transition state and electron transfer occurs to acceptor molecules. This electron transfer process competes with fluorescence from the donor's excited state. The forward electron transfer rate is

$$K_f(R) = 1/\tau \exp((R_0 - R)/a_f),$$

where R is the donor–acceptor-separation, R_0 is the distance at which forward transfer has the same probability as fluorescence, and a_f is related to the overlap of the donor and acceptor wave functions.[8,17,36]

The solvent shells around the newly formed ion pairs begin relaxing to their equilibrium structures. The reorientation of the solvent dipole moments lowers the energy of the ions and increases the energy of the neutral states. As a result, the solvent relaxation increases the barrier height for electron back transfer which reduces the electron back transfer rate. In the model the time scale for the internal, relaxation, vibrational redistribution, and thermalization of the ions ($\chi_0 \rightarrow \chi_\infty$) is taken to be short (10–100 fs) compared to the time scale for solvent relaxation (several hundred femtoseconds to many picoseconds). This assumption may not always hold. In some solvents, the time for thermalization could be comparable to the time for solvent relaxation. The theoretical framework presented below can be extended to include this case. To simplify the calculation of the observables it is assumed that solvent relaxation shifts the potential curves of the neutral ground state and neutral excited state of the donor molecule approximately the same amount. This is generally true for nonpolar molecules such as antracene or rubrene. Solvent relaxation due to the donor electronic excitation is neglected. Compared to the formation of the ions, the effects of the excited state on the solvent structure is not significant for neutral donors which do not possess dipole moments which change substantially upon excitation. The influence of solvent relaxation about the excited donor on forward electron transfer can be treated in a manner which is analogous to the method used to describe the effect of solvent relaxation on back transfer presented below.

For electron transfer at fixed distance, Sumi and Marcus[33] developed a theory for the electron transfer rate that included the dynamical effects of solvent relaxation. Two of the limiting cases they studied were electron transfer faster and slower than the time scale for solvent relaxation. In our model for intermolecular electron transfer, after ion formation there is a distribution of distances between the newly created ion pairs. Close pairs will recombine quickly and pairs further away will recombine slowly or on the same time scale as solvent relaxation. The important feature of the theory presented here is to properly perform the spatial averaging including the effects of solvent relaxation on the time dependence of the electron transfer rate.

In the next three sections the details of the calculation will be presented. Section A gives the derivation of the cation distribution function over the solvent states, the effective back transfer rate, and the cation probability when the cation is formed at $t = 0$ for a single donor acceptor pair with separation R. Section B generalizes the cation probability function derived in Sec. A so that the probability function also contains ions formed at times determined by the finite forward transfer rate. The cation probability is then ensemble averaged over the donor–acceptor separations in Sec. C.

A. The effective back transfer rate

In the model, the forward electron transfer initially populates the internal and external states χ_0 and q_0, respectively. Following ultrafast relaxation of the internal molecular degrees of freedom, the mechanical degrees of freedom of the solvent about the ions have not yet relaxed and are in state q_0. Subsequent solvent relaxation takes the ions to a more stable state q_∞ in which the solvent contribution to the barrier height is $\Delta q = q_0 - q_\infty$. During the solvent relaxation process the electron back transfer rate is significantly modified. The model for the solvent relaxation process can be summarized as: (a) the energies of the ion–solvent systems are shifted and the rate of the shifts can be described by the solvent relaxation parameter τ_r, the relaxation time, and (b) there is a population distribution over different solvent states that spreads as a function of time described by an energy diffusion parameter, D. A single solvent relaxation parameter, τ_r, is used because it is sufficient to display the important features of the effect of solvent relaxation on back transfer. In many physical systems it is a reasonable approximation. The theoretical treatment is general, and can be readily extended to any time dependence of the solvent relaxation. As a subensemble of ions that are created at a particular time relax, interactions with the heat bath cause random fluctuations up and down in energy. This is in addition to the net down hill motion. The result is a packet that spreads as it moves from q_0 toward q_∞, the energies which are characteristic of the initial and final solvent states. The forward electron transfer can place the ions in a distribution of solvent states about q_0. Since q_0 is a characteristic of the thermally accessible transition state, the distribution is most likely narrow. We have not included a distribution about q_0 but it can be taken into account.

We first consider a single donor and a single acceptor. The separation between the donor and acceptor is denoted by R. Initially we take the forward transfer rate to be infinitely fast so that the cations are formed at $t = 0$.

To study the evolution of the cation probability, the function $Q_{ct}(q,R,t)$ is defined such that $Q_{ct}(q,R,t)dq$ is the probability of finding the system (cation, anion, and solvent) within the range of solvent states $[q,q+dq]$. The total cation probability can be written as

$$Q_{ct}(R,t) = \int Q_{ct}(q,R,t)dq. \tag{1}$$

According to the model described in the last two paragraphs, at time $t = 0$, the forward transfer prepares all the systems in the unrelaxed solvent state q_0. Therefore

$$Q_{ct}(R,t=0) = 1. \tag{2}$$

At longer times some ions have recombined due to electron back transfer and

$$Q_{ct}(R,t>0) < 1. \tag{3}$$

The number of cations which have returned to the neutral ground state because of electron back transfer in the time interval $[t,t+dt]$ and energy $[q,q+dq]$ is given by the following expression

$$K_b(q,R)Q_{ct}(q,R,t)dqdt, \tag{4}$$

where $K_b(q,R)$ is the electron back transfer rate. We now define a normalized cation probability distribution function $f(q,t)$

$$Q_{ct}(q,R,t) = Q_{ct}(R,t)f(q,t). \tag{5}$$

Integrating both sides of Eq. 5 and using Eq. 1 we obtain

$$\int f(q,t)dq = 1. \tag{6}$$

$f(q,t)$ is the conditional probability for the solvent state to have the value q at time t if at $t = 0$ it had the energy q_0.

As indicated by Eqs. (4) and (5), the total number of cations which returned to the neutral ground state in the time interval $[t,t+dt]$ can be obtained by integrating over q.

$$dQ_{ct}(R,t) = -\left[\int K_b(q,R)f(q,t)dq\right]Q_{ct}(R,t)dt, \tag{7}$$

where the term in the brackets is the effective electron back transfer rate, $K_{\text{eff}}(\text{R,t})$, and depends on the donor–acceptor separation and the time.

$$K_{\text{eff}}(R,t) = \int K_b(q,R)f(q,t)dq. \tag{8}$$

$K_{\text{eff}}(R,t)$ is the back transfer rate averaged over solvent states at a time t and separation R. At time $t = 0$, $f(q,t=0) = \delta(q-q_0)$ and $K_{\text{eff}}(R,t=0) = K_b^0(R,T)$. At $t > 0$ the solvent state relaxes to a more stable configuration q and the back transfer rate slows down. Therefore $K_{\text{eff}}(R,t) < K_{\text{eff}}(R,t=0)$. Rearranging Eq. (7) we obtain the differential equation for $Q_{ct}(R,t)$

$$\frac{dQ_{ct}(R,t)}{dt} = -K_{\text{eff}}(\text{R,t})\text{Q}_{\text{ct}}(\text{R,t}). \tag{9}$$

The solution for Eq. (9) with the initial condition $Q_{ct}(R,t=0) = 1$ is

$$Q_{ct}(R,t) = \exp\left(-\int_0^t K_{\text{eff}}(R,t')dt'\right). \tag{10}$$

We shall now examine the function $f(q,t)$ in some detail. For simplicity we use the Debye model for the solvent relaxation. This leads to the well-known result that the relaxation of the solvent polarization is exponential with a decay time equal to τ_r. As a consequence, the change in the solvent energy is given by[35]

$$q(t) = q_\infty + \Delta q \exp(-t/\tau_r), \tag{11}$$

where $q(t)$ is the solvent energy at time t, q_∞ is the solvent energy for the relaxed solvent state, and $\Delta q = q_0 - q_\infty$ is the solvent contribution to the back transfer barrier height.

The solvent relaxation can be viewed as a diffusion process in energy space. In a reasonable approximation the probability distribution function $f(q,t)$ satisfies the Fokker–Planck equation[43]

$$\frac{\partial f(q,t)}{\partial t} = \left[\frac{1}{\tau_r}\frac{\partial(q-q_\infty)}{\partial q} + D\frac{\partial^2}{\partial q^2}\right] f(q,t), \tag{12}$$

where D is a diffusion constant for motion in energy space due to random fluctuations of the solvent. The solution of Eq. (12) is a Gaussian distribution function moving in time. This is the same as Sparpaglione and Mukamel's propagator of the solvation coordinate [our Eq. (13) is the same as Sparpaglione and Mukamel's Eq. (D8) with $\delta_m = q_\infty$, $M_m(t) = \exp(-t/\tau_r)$, and $\Delta^2 = D\tau_r$].[27] Mukamel's propagator of the solvent coordinate is not limited to the Debye model. Thus, if necessary, $f(q,t)$ can be extended to include non-Debye solvents. Since at $t=0$ the ions are in the q_0 solvent state $f(q_0,t=0) = \delta(q-q_0)$. For $t>0$ the distribution is

$$f(q,t) = \frac{\exp\left(-\dfrac{[q-q(t)]^2}{2D\tau_r(1-\exp(-2t/\tau_r))}\right)}{\sqrt{2\pi D\tau_r[1-\exp(-2t/\tau_r)]}}. \tag{13}$$

With $f(q,t)$ it is possible to evaluate the time dependent electron back transfer rate, $K_{\text{eff}}(R,t)$. The electron transfer rate has two parts. One depends on the donor–acceptor separation which represents the overlap of the donor and acceptor wave functions. The other part depends on the potential barrier height separating the ion and neutral state. The barrier height has contributions from the internal degrees of freedom and the solvent degrees of freedom. We have a assumed a separation of time scales. The relaxation of the internal degrees of freedom is much faster than the solvent relaxation. Therefore, immediately following electron transfer the internal degrees of freedom have relaxed and determine the initial barrier height for electron back transfer. This barrier height is not explicitly shown but is contained in $K_b^0(R,T)$ which is the distance dependent rate constant for electron back transfer prior to solvent relaxation. $K_b^0(R,T)$ depends on the temperature, T, because it contains the internal contribution to the back transfer barrier height. We write the solvent contribution to the barrier height dependence of the back transfer rate in the exponential form.[1,2,21] Therefore,

$$K_b(q,R) = \exp(-(q_0-q)/kT)K_b^0(R,T), \tag{14}$$

where $K_b^0(R,T)$ depends on the donor–acceptor separation and the temperature. The electron back transfer rate for the unrelaxed solvent state q_0 is defined as

$$K_b^0(R,T) = \frac{1}{\tau}\exp((R_b^0 - R)/a_b^0), \tag{15}$$

where R_b^0 and a_b^0 are the electron transfer parameters for solvent configuration q_0. With Eqs, (14), (13), and (8) we obtain the effective back transfer rate

$$\begin{aligned} K_{\text{eff}}(R,t) = {} & K_b^0(R,T)\int_{q_0}^{\infty} f(q,t)dq \\ & + \int_{q_\infty}^{q_0} K_b(q,R)f(q,t)dq \\ & + K_b(q_\infty,R)\int_{-\infty}^{q_\infty} f(q,t)dq, \end{aligned} \tag{16}$$

where the first term represents the rate from population in the q_0 solvent state, the second term is for population in the states between q_0 and q_∞, and the third term is the rate contribution from population in the lowest solvent state. The first and third integrals account for the mathematical spread of the Gaussian past the physical limits, q_0 and q_∞. At $t=0$ the distribution function becomes a delta function at q_0 thus we obtain

$$\begin{aligned} K_{\text{eff}}(R,t=0) &= \int_{-\infty}^{\infty} K_b(q,R)\delta(q-q_0)dq \\ &= K_b^0(R,T). \end{aligned} \tag{17}$$

The integration in Eq. (16) can be carried out. The result is

$$\begin{aligned} K_{\text{eff}}(R,t) = {} & K_b^0(R,T)\frac{1}{2}[\text{erf}(Z\Delta q(\exp(-t/\tau_r)-1))+1] \\ & + K_b(q_\infty,R)\frac{1}{2}[1-\text{erf}(Z\Delta q\exp(-t/\tau_r))] \\ & + K_b^0(R,T)\frac{1}{2}\exp(-\Delta q/kT) \\ & \times\exp\left(\frac{\Delta q\exp(-t/\tau_r)}{kT}+P^2\right) \\ & \times[\text{erf}(Z\Delta q\exp(-t/\tau_r)+P) \\ & - \text{erf}(Z\Delta q(\exp(-t/\tau_r)-1)+P)], \end{aligned} \tag{18}$$

where $\text{erf}(x)$ is the standard error function, with

$$P = \sqrt{\frac{D\tau_r(1-\exp(-2t/\tau_r))}{2(kT)^2}}, \tag{18a}$$

$$Z = \frac{1}{\sqrt{2D\tau_r(1-\exp(-2t/\tau_r))}}. \tag{18b}$$

Equation (18) has some interesting limits. At infinitely fast relaxation, the solvent is relaxed on the time scale of electron back transfer. This is also the case at times long compared to the relaxation time and the spreading of the distribution over solvent states. In this limit Eq. (19) is time independent and can be simplified to

$$\begin{aligned} K_{\text{eff}}(R) &= K_b^0(R,T)\exp(-\Delta q/kT) \\ &= \frac{1}{\tau}\exp(-\Delta q/kT)\exp((R_b^0-R)/a_b^0). \end{aligned} \tag{19}$$

From Eq. (19) we see that R_b^0 and a_b^0 are related to R_b and a_b, which are the electron transfer parameters in the long time limit, by the following relations:

$$a_b^0 = a_b, \tag{19a}$$

$$R_b^0 = R_b + a_b\frac{\Delta q}{kT}, \tag{19b}$$

a_b parameterizes the rate of the exponential fall off of the cation–anion wave functions' overlap. This factor determines the distance dependence of the electronic part of the electron transfer matrix element. In the framework of this model, a_b is unaffected by solvent relaxation. Rather, solvent relaxation changes R_b, which parameterizes the magnitude of the overlap. a_b and R_b can be determined by experiments conducted on a time scale which is long compared to τ_r. This has been done for the rubrene–duroquinone system using transient grating experiments.[39] As will be discussed in more detail below, a short time scale experiment can determine R_b^0, and through Eq. (19b), Δq, the contribution of solvent relaxation to the barrier for electron back transfer can also be determined.

Under the limit of $D \to 0$ (no spreading of the packet as it relaxes) the effective rate becomes

$$K_{\text{eff}}(R,t) = K_b^0(R,T)\exp(-\Delta q/kT) \times \exp\left(\frac{\Delta q}{kT}\exp(-t/\tau_r)\right), \tag{20}$$

this is equivalent to having the delta-function form in the population distribution $f(q,t)$ in Eq. (13)

$$f(q,t) = \delta(q - q(t)). \tag{21}$$

Using $K_{\text{eff}}(R,t)$, the cation state population probability, given in Eq. (18), $Q_{ct}(R,t)$ from Eq. (10), can be evaluated. $Q_{ct}(R,t)$ is the probability that the donor is a cation for a single donor acceptor pair, at a distance R, with an infinitely fast forward transfer rate (used here so that all of the ions are created at the same time, $t = 0$) and a back transfer rate that depends on solvent relaxation. In the next section this result is generalized for the case of a finite forward transfer rate.

B. Generalization of $Q_{ct}(R,t)$

The generalization of the result obtained in Sec. A for $Q_{ct}(R,t)$ for a finite forward transfer rate is straight forward. As in Sec. A, at this point in the development there is a single donor and a single acceptor. At $t = 0$ the donor molecule is optically excited. At some later time t_1, the excited donor transfers an electron to the acceptor molecule.

The decay of the donor excited state is due to the donor relaxation to the ground state (fluorescence and radiationless relaxation) and electron transfer (see Fig. 1). The probability that the donor molecule is in the excited state at a later time t is

$$P_{ex}(R,t) = \exp(-t/\tau)\exp(-K_f(R)t), \tag{22}$$

with the initial condition $P_{ex}(R,t=0) = 1$. The probability for forward transfer occurring in the interval $[t_1, t_1 + dt_1]$ is $K_f(R)P_{ex}(R,t_1)dt_1$. This transfer generates a cation. The survival probability for the cation generated at time t_1 is

$$dP_{ct}(R,t) = K_f(R)P_{ex}(R,t_1)Q_{ct}(R,t-t_1)dt_1. \tag{23}$$

Where $Q_{ct}(R,t-t_1)$ is the cation survival probability at t for unit forward transfer at t_1 and is given in Eq. (10). Therefore the total probability of finding a cation at time t with an anion at distance R is given by the integral over all formation times t_1 from zero to t in Eq. (23).

$$P_{ct}(R,t) = \int_0^t K_f(R)P_{ex}(R,t_1)Q_{ct}(R,t-t_1)dt_1. \tag{24}$$

Equation (24) satisfies the initial condition that at $t = 0$ the donor molecule is in its excited state and $P_{ct}(R,t=0) = 0$.

C. Many particles and the ensemble average

For randomly distributed donors and acceptors the spatial ensemble average including the effects of donor–acceptor and acceptor–acceptor excluded volume has been performed previously.[37] Here a brief description of the method will be given. In the previous treatment, solvent relaxation at short time was not considered, and the back transfer rates were distance dependent but time independent. In this section the spatial ensemble average using the time dependent effective back transfer rate is performed to obtain the ensemble averaged time dependent cation probability.

The excited state survival probability, $P_{ex}(R_1,...,R_n,t)$, and the cation probability when the ith acceptor becomes the anion are

$$P_{ex}(R_1,...,R_n,t) = \exp(-t/\tau)\exp\left(-\sum_{j=1}^{n} K_f(R_j)t\right), \tag{25}$$

$$P_{ct}^i(R_1,...,R_n,t) = \int_0^t K_f(R_i)P_{ex}(R_1,...,R_n,t_1) \times Q_{ct}(R_i,t-t_1)dt_1. \tag{26}$$

Since the back transfer process involves only two particles, the cation and anion, $Q_{ct}(R_i,t-t_1)$ in Eq. (26) only depends on R_i, the ion separation. The dependence on the other acceptors in $P_{ct}(R_1,...,R_n,t)$ is contained in the details of the forward transfer.[37]

To account for the random distribution of the acceptor molecules, the probabilities given by Eqs. (25) and (26) need to be ensemble averaged over all possible acceptor configurations. The ensemble average of $P_{ex}(R_1,...,R_n,t)$ was derived by Inokuti and Harayama[36] and was generalized by Blumen and Manz to include donor–acceptor and acceptor–acceptor excluded volume effects.[44] To calculate the ensemble average of $P_{ct}(R_1,...,R_n,t)$ the method in Ref. 37 was used. Since the spatial distribution of the acceptors at different points is uncorrelated and the ensemble averaging procedure is independent of time integration, the ensemble average of Eq. (26) over all acceptors except the ith one is

$$\langle P_{ct}^i(R_i,t)\rangle_{n-1} = \int_0^t K_f(R_i)\langle P_{ex}(R_i,t_1)\rangle_{n-1} \times Q_{ct}(R_i,t-t_1)dt_1, \tag{27}$$

where $\langle\rangle_{n-1}$ denotes an average over the spatial coordinates except the spatial coordinate of the ith acceptor. $\langle P_{ct}(R_i,t)\rangle_{n-1}$ is the averaged probability of finding the donor in its cation state with an anion at R_i. $\langle P_{ex}(R_i,t_1)\rangle_{n-1}$ in the thermodynamic limit is[37]

$$\langle P_{ex}(R_i,t)\rangle = \exp(-t/\tau)\exp(-K_f(R_i)t) \times \exp\left(\frac{-4\pi}{d^3}\sum_{k=1}^{\infty}\frac{P^k}{k}\int_{R_m}^{\infty} \times [1-\exp(-K_f(R_j)t)]^k R_j^2 dR_j\right), \tag{28}$$

where d is the acceptor diameter, R_m is the sum of the donor

and acceptor radii, $P = Cd^3$, and C is the acceptor concentration. Equation (28) included donor–acceptor and acceptor–acceptor excluded volume effects. A simpler expression is obtained when excluded volume is not taken into account.[37] This result can be obtained by setting R_m and d to zero. The physical meaning of Eq. (27) can be understood as follows: $K_f(R_i)\langle P_{ex}(R_i,t_1)\rangle_{n-1}$ is the rate of an excited donor transferring an electron at time t_1 to an acceptor at R_i. Only some of these ions will remain at a later time t. The survival probability is given by $Q_{ct}(R_i,t-t_1)$. The total probability of finding a cation at time t with an anion at position R_i is the product of these two terms integrated over all the times from zero to t.

Finally the total time dependent probability of a donor molecule being a cation, $\langle P_{ct}(t)\rangle$, is found by averaging over the last spatial coordinate R_i and summing over all acceptors, and then taking the thermodynamic limit. The result is

$$\langle P_{ct}(t)\rangle = 4\pi C \int_{R_m}^{\infty} \langle P^i_{ct}(R_i,t)\rangle R^2 dR, \tag{29}$$

where $\langle P^i_{ct}(R_i,t)\rangle$ is given by Eq. (27) using the thermodynamic limit of $\langle P_{ex}(R_i,t)\rangle_{n-1}$ given in Eq. (28). In Eq. (27), $Q_{ct}(R,t)$ is given in Eq. (10) using $K_{\text{eff}}(R,t)$ given in Eq. (18).

Using the forms of the forward transfer rate, $K_f(R)$, the excited state population probability $\langle P_{ex}(t)\rangle$, and the effective back transfer rate $K_{\text{eff}}(R,t)$, the ensemble averaged cation probability $\langle P_{ct}(t)\rangle$ is readily evaluated numerically. In the next section we shall discuss some interesting properties of $\langle P_{ct}(t)\rangle$ and use it to calculate the transient grating observable.

III. NUMERICAL RESULTS AND DISCUSSION

In the previous section we obtained the expression for the time dependent effective electron back transfer rate, $K_{\text{eff}}(R,t)$. This accounts for the effect on electron back transfer of solvent reorganization that takes place after forward transfer. The time dependent probabilities that a donor is in its excited state, and cation state are also given. Numerical evaluations of these probability functions and the effective electron back transfer rate will be carried out in this section. These calculations will provide a detailed physical picture of the influence of the time dependent solvation process on the back transfer dynamics.

A. Electron back transfer rate

As given in Eq. (18), the effective electron back transfer rate depends on the solvent relaxation time, τ_r, the change in the back transfer barrier height Δq, the energy diffusion parameter D, and the electron back transfer parameters of the unrelaxed solvent state a_b^0, and R_b^0. In the model, these parameters are taken to be independent of distance, and the ensemble average over distance involves the forward and back transfer rates only. It is possible that the parameters are in fact distance dependent.[45] Adding a distance dependence to the above parameters is tractable because it does not change the formalism given in Sec. II. The nature of the results given below will not be affected by the inclusion of distance dependent solvent relaxation parameters.

In the calculation, the electron transfer reaction is taken to occur in the normal free energy region,[21] i.e., the back transfer rate decreases as the solvent relaxes. This simplifies the expression for the back transfer rate that takes into account the barrier height change due to solvent relaxation. A more general approach would be to express the back transfer rate, using the Marcus' result,[21] as

$$K_b(\lambda,R) = \exp(-\Delta G^*/kT)S(R), \tag{30a}$$

$$\Delta G^* = \frac{(\lambda + \Delta G^0)^2}{4\lambda}, \tag{30b}$$

rather than Eq. (14). Where $S(R)$ contains the electron transfer matrix element and is distance dependent. λ is the reorganization energy which includes a solvent part related to our Δq and a part due to internal relaxation which is not explicitly included in our model but rather contained in the parameter R_b^0. To include this generalization another parameter, ΔG^0, which is the standard free-energy change for the electron transfer must also be determined.[26] Equation (30) takes care of the normal and inverted free-energy region transfer dynamics. Two limiting cases can be distinguished depending on the relative magnitudes of λ and ΔG^0. When $-\Delta G^0 < \lambda$ (normal free energy region) K_b will decrease with increasing λ, when $-\Delta G^0 > \lambda$ (inverted free energy region), K_b will increases with increasing λ. The calculations presented here can be modified to handle the inverted region.

The calculation of the effective electron back transfer rate as a function of time (after the forward electron transfer) for various solvent parameters, τ_r, Δq, and D are presented in Figs. 2–4. For these calculations the temperature of the system is 200 cm^{-1} (kT about room temperature), and the excited state life time, which is used to scale the rate, is 16 ns (16 ns is rubrene's life time, which is similar to many other excited singlet states of aromatic hydrocarbons). The other parameters are given in the figure captions for each curve. Figure 2 plots the effective back transfer rate for various solvent relaxation times. One observes that $K_{\text{eff}}(R,t)$ drops rapidly when $t < \tau_r$, and then becomes constant as time increases. Immediately following the forward electron transfer ($t = 0$) the system is in an unrelaxed solvent state, q_0 (but relaxed internal state χ_∞), and the electron back transfer rate is extremely high. At longer time the solvent reorganization stabilizes the ions relative to the neutrals and decreases the electron back transfer rate. Figure 2 also shows that $K_{\text{eff}}(R,t)$ is steeper for faster solvent relaxation times. As τ_r approaches zero a greater fraction of back transfer events occur from relaxed solvent configurations. The figure also demonstrates that at times long compared to τ_r, it is sufficient to consider time independent but distance dependent back transfer rates.

Figure 3 displays the effective back transfer rate $K_{\text{eff}}(R,t)$ for various Δq's. The solvent relaxation time is 10 ps. Like Fig. 2 these curves decrease rapidly at early time and are constant at long time. As Δq increases, the shape of $K_{\text{eff}}(R,t)$ at short time becomes steeper and the back transfer rate from the relaxed solvent state decreases exponential-

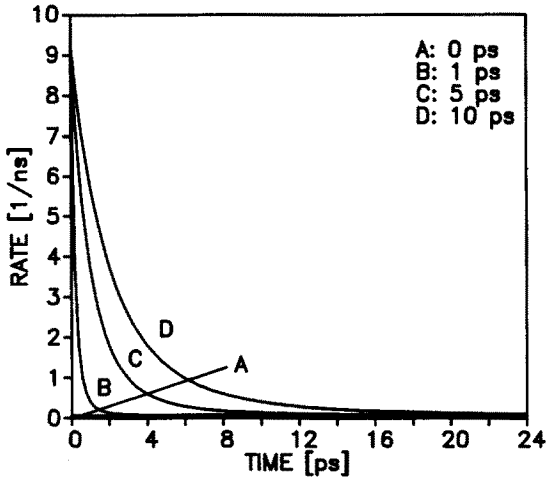

FIG. 2. The effective back transfer rate. The distance is 11 Å. The other parameters are $\Delta q = 5kT$, $D = 100\,\mathrm{cm}^{-2}/\mathrm{ps}$, $kT = 200\,\mathrm{cm}^{-1}$, $a_b^0 = 1.0$ Å, and $R_b^0 = 16.0$ Å. Curve A is a constant with the value $0.0625\,\mathrm{ns}^{-1}$. When $t < \tau_r$, the rate drops rapidly. At times much greater than τ_r the rate is a constant.

ly as a function of Δq. For $\Delta q = 0$, the effective back transfer rate is time independent, i.e., $K_{\mathrm{eff}}(R,t) = K_b^0(R,T)$.

The dependence of the effective back transfer rate on the energy diffusion parameter D is plotted in Fig. 4. In the Fig. τ_r is varied from 0 to 25 ps. For each relaxation time two curves were calculated, one with $D = 0$ and the other with $D = 1000\ \mathrm{cm}^{-2}/\mathrm{ps}$ (energy squared per unit time). The barrier height change Δq is 5 kT. As discussed in the previous section, $D = 0$ corresponds to δ-function relaxation (all sites relax together). When $D = 1000\ \mathrm{cm}^{-2}/\mathrm{ps}$ the width of the solvent distribution is on the order of kT or larger (the width of the distribution also depends on τ_r and the time). The full width at half maximum of the distribution is

$$\mathrm{FWHM} = \sqrt{8\ln(2)D\tau_r[1-\exp(-2t/\tau_r)]}. \quad (31)$$

It is important to mention that D can be expressed as $D = \Delta^2/\tau_r$,[27] where Δ is related to the dielectric properties of the solvent. Thus, in principle there is only one characteristic solvent time, τ_r. In more complex situations, this relationship may not hold. Therefore we have kept D as an independent parameter. Figure 4 indicates that for parameters similar to those measured in experiments,[39] the effective electron back transfer rate is not very sensitive to the value of the diffusion parameter, D. Only when the relaxation time becomes long do significant variations in the rate occur. For the parameters used in the calculation of Fig. 4 significant differences due to different diffusion parameters appear beginning at $\tau_r = 25$ ps. These differences arise because for slow relaxation rates and large D the population is relaxing very slowly yet because of the large diffusion parameter, a significant part of the population is spreading downward rapidly away from the slowly moving center of the population. Thus when the relaxation time is fast compared to the spreading of the population, it is possible to use the δ-function form of the cation distribution function as an approximation to the actual distribution when comparing this theory to data.

B. Cation probabilities

Calculations of the ensemble averaged time evolution of the cation probability are presented in this section. The time dependent cation probability can be looked at in several ways. For a system of randomly distributed donors and acceptors, it is possible to look at the influence of a particular acceptor on the cation probability as a function of time and donor–acceptor separation. To investigate the effect of the ith acceptor, it is necessary to average over the positions of all other acceptors, since they in part determine the rate of electron transfer to the ith acceptor when it is at location R_i. This has been done before without solvent relaxation.[37,39] The expression including solvent relaxation effects is given by $\langle P_{ct}^i(R_i,t)\rangle$ in Eq. (27) [with $\langle P_{ex}(R_i,t)\rangle$ in the thermo-

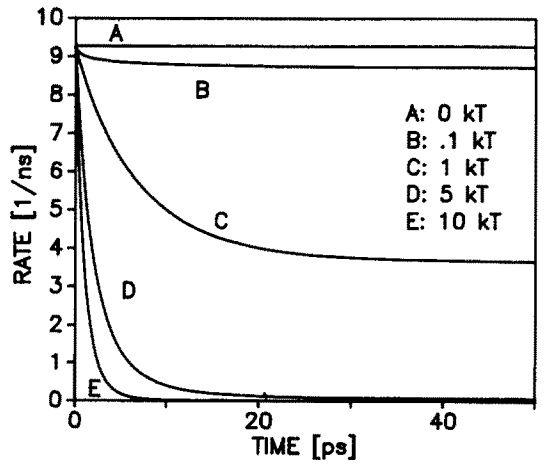

FIG. 3. The effective back transfer rate as a function of time and Δq. The other parameters are the same as in Fig. 2. As Δq increases the stability of the ions increases and the back transfer rate decreases.

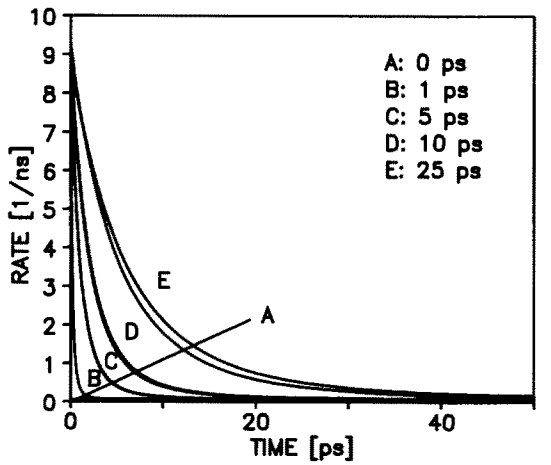

FIG. 4. The effective back transfer rate as a function of time, D, and τ_r. For each relaxation time two curves were calculated one with $D = 0$ and the other with $D = 1000\ \mathrm{cm}^{-2}/\mathrm{ps}$. Curve A is a constant with the value $0.0625\ \mathrm{ns}^{-1}$. Note the insensitivity to changes in D when τ_r is short.

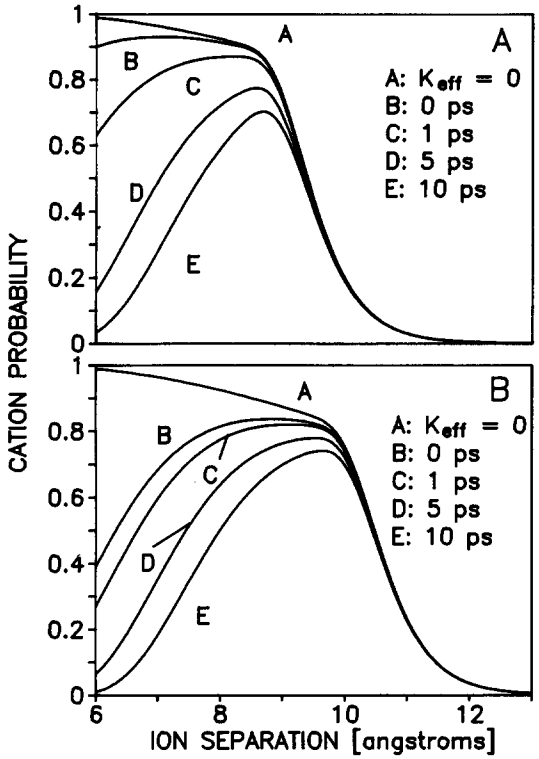

FIG. 5. The probability the donor is a cation as a function of the ion separation and τ_r. The parameters are $R_m = 6$ Å, $d = 7.2$ Å, $a_f = 0.5$ Å, $R_0 = 13$ Å, $a_b^0 = 1$ Å, $R_b^0 = 16$ Å, $\tau = 16$ ns, $\Delta q = 5kT$, $D = 100$ cm^{-2}/ps, $KT = 200$ cm^{-1}, and the acceptor concentration $C = 0.1$ M. In A. $t = 10$ ps and B. $t = 100$ ps. At long distance all curves have the same value. For comparison, the top curve in A and B have $K_{eff}(R,t) = 0$ (no back transfer).

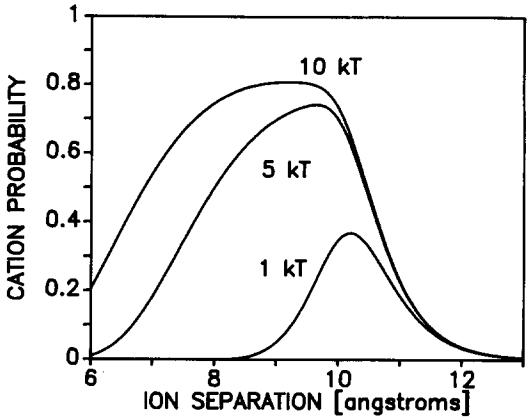

FIG. 6. The probability the donor is a cation as a function of the ion separation and Δq. The parameters are the same as in Fig. 5 with $\tau_r = 10$ ps and $t = 100$ ps. At long distance all curves have the same value. The curves show that as the ionic state stability increases (increasing Δq) the cation probability increases.

dynamic limit given in Eq. (28)]. Cross sections of this two-dimensional surface as a function of distance at various times and solvent relaxation parameters are shown in Figs. 5, and 6.

$\langle P_{ct}^i(R_i,t)\rangle$ versus distance for a unit volume element about R_i is displayed in Fig. 5 for solvent relaxation times varying from 0.0 to 10 ps and for $K_{eff}(R,t) = 0$. In Fig. 5a the time is 10 ps after the formation of the excited states, while Fig. 5b is at $t = 100$ ps. In each curve $\Delta q = 5kT$. The other parameters are $a_f = 0.5$ Å, $a_b^0 = 1.0$ Å, $R_0 = 13$ Å, $R_b^0 = 16$ Å, and the concentration of acceptors is 0.1 M. The excited state lifetime is 16 ns. The shortest distance is 6 Å because of donor–acceptor excluded volume. The probability of finding a cation with an anion at a given distance from it decreases as the solvent relaxation time increases. Increased τ_r means the solvent relaxation is slower and the ions have a faster recombination rate for a longer period of time. As a result, the electron back transfer rate increases and the cation probability decreases. Figure 5 also shows that the differences in the cation probabilities for various τ_r's become smaller as the ion pair separation increases or time increases. All the curves seem to coalesce at long distance. For the parameters used in the calculation, at long distance the forward transfer rate is larger than the back transfer rate, $K_{eff}(R,t)$. This means at long distance the ion population is controlled by the forward transfer rate for the two times used in Fig. 5. In the figure $\langle P_{ct}(R_i,t)\rangle$ was also calculated for $K_{eff}(R,t) = 0$ (top curve in Figs 5a and b). As can be seen at long distance it coalesces with the other curves. If the $K_{eff}(R,t)$ were chosen to be larger there would be a greater difference between the curves at long distance. This is demonstrated in Fig. 5 at short distances, where $K_{eff}(R,t) > K_f(R)$; all the curves differ significantly.

Figure 6 shows the dependence of $\langle P_{ct}^i(R_i,t)\rangle$ on the cation–anion separation, and on Δq varying from 1 to 10 kT. The other parameters are the same as those used in Fig. 5. $\tau_r = 10$ ps and the time is 100 ps. Like Fig. 5 these curves display the cation probability for various cation–anion separations at a given time, and shows how the distribution changes as Δq changes. As Δq increases more ions will survive at a given time and distance. For example, at 100 ps the ion pairs with 8 Å separations have recombined with $\Delta q = 1kT$. However, ions will have a higher survival probability at $\Delta q = 5kT$. The greater extent of the solvent relaxation (large Δq) stabilizes the ions and substantially reduces the electron back transfer rate.

The total time dependent probability of a donor molecule being a cation for all ion separations was found by averaging over the last spatial coordinate R_i, and summing over all acceptors as given in Eq. (29). The numerical evaluation of $\langle P_{ct}(t)\rangle$ as a function of time for various electron transfer and solvent parameters are plotted in Figs. 7 and 8.

Figure 7 shows the ensemble averaged time evolution of the cation probability $\langle P_{ct}(t)\rangle$ for various solvent relaxation times. R_0, R_b^0, a_f, a_b, and the fluorescence lifetime are same as those used in Figs. 5, and 6. The values of these parameters are similar to those found in the literature.[39] One observes that $\langle P_{ct}(t)\rangle$ rises rapidly within the first 100 ps, reaches its maximum value, and then slowly decays to zero. At $t = 0$, the donor molecules are in the excited state, and no ion pairs exist. After excitation, a fraction of the donors in the ensemble will fluoresce and a fraction will undergo forward electron transfer. As a result of electron transfer, the ion state population builds up. The onset of ion pair formation marks

the beginning of the solvent relaxation process and electron back transfer. The competition between these processes determines the shape of $\langle P_{ct}(t)\rangle$. The curves plotted in Fig. 7 demonstrate that the cation probability increases as τ_r decreases. At short time, the curves with different solvent relaxation times have very different shapes. As time increases, more ions reach their relaxed solvent state and back transfer occurs from more stable configurations. At long time, differences due to τ_r in $K_{\text{eff}}(R,t)$ become smaller and the cation probability curves with different τ_r's have the same shape. This property is important for determining the solvent relaxation parameters τ_r and Δq experimentally. In the next subsection, we will discuss how these parameters can be extracted from experimentally measured quantities.

Figure 8 shows the dependence of $\langle P_{ct}(t)\rangle$ on time for different Δq's varying from 1 to 10 kT. The solvent relaxation time is 10 ps and the other parameters used in the calculation are the same as in Fig. 7. The curves in Fig. 8 are analogous to those in Fig. 7. The parameter Δq is closely related to the solvent polarity. As Δq increases, the height of the solvent contribution to the barrier which must be surmounted for back transfer to occur increases. By increasing Δq the rate of back transfer is greatly reduced and the cation probability will increase.

The dependence of $\langle P_{ct}(t)\rangle$ on R_0, a_f, R_b, and a_b in the absence of solvent relaxation is discussed in Ref. 27.

C. Experimental observables

The dynamics of electron transfer and back transfer are determined by five molecular parameters, the concentration of the acceptors, and three solvent relaxation parameters. Besides the donor excited state lifetime τ, there are four molecular parameters, a_f and R_0 (forward transfer parameters), and a_b and R_b (back transfer parameters for relaxed solvent). The three solvent dependent parameters are the solvent relaxation time τ_r, the difference in the activation barrier height before and after the solvent relaxation, Δq, as well as the energy diffusion parameter D. The life time of the donor excited state can be directly measured from a sample without acceptor molecules present. The forward transfer parameters can be determined by a combination of concentration dependent steady state fluorescence quenching and time-resolved fluorescence quenching experiments.[12,17,36,39] With these parameters, the back transfer parameters and solvent relaxation parameters can be obtained from a ground state recovery experiment. The most common ground state recovery method is a pump-probe experiment. Pump-probe experiments, however, generally have problems with dynamic range because it is necessary to measure a small change in a large signal. Here we will consider the transient grating experiment. This is a zero background technique which helps avoid a variety of artifacts which can occur in a probe pulse experiment.[39] The back transfer parameters and the solvent parameters can be extracted from the transient grating observable. The transient grating experiment and its use in measuring electron transfer parameters has been discussed previously.[39]

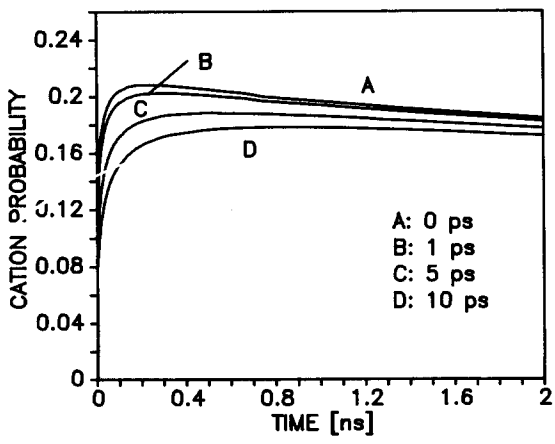

FIG. 7. The total cation probability as a function of time and τ_r, $\Delta q = 5kT$, and the other parameters are the same as in Fig. 5. The cation probability decreases as τ_r increases. As τ_r increases it takes longer for the solvent to relax.

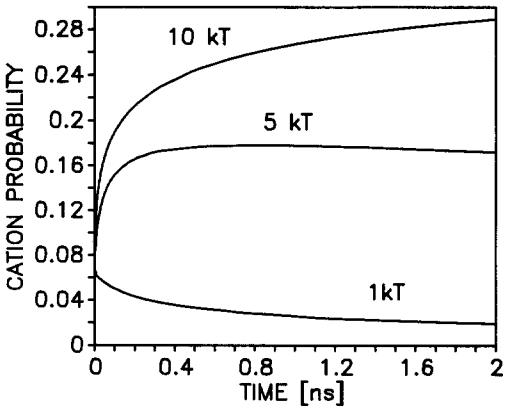

FIG. 8. The total cation probability as a function of time and Δq. $\tau_r = 10$ ps, and the other parameters are the same as in Fig. 5. As the ion stability increases (Δq increases) the cation probability increases.

The transient grating observable, $S(t)$, is proportional to the square of the peak-null difference in the complex index of refraction of the medium.[46] The change in the index arises from the reduction in the ground state population in the grating peaks because of the formation of ion pairs, and donor excited states. $S(t)$ is given by

$$S(t) = A(\langle P_{ex}(t)\rangle + \langle P_{ct}(t)\rangle)^2. \tag{32}$$

Equation 32 shows the connection between the transient grating signal and the electron transfer parameters. The first term $\langle P_{ex}(t)\rangle$ is determined by concentration dependent steady-state fluorescence quenching and time-resolved fluorescence quenching experiments. The extraction of the donor's excited state lifetime, and forward transfer parameters is straight forward and has been discussed elsewhere.[12,17,36,39] The electron back transfer parameters a_b and R_b and the solvent relaxation parameters τ_r, D, and Δq, that enter into $\langle P_{ct}(t)\rangle$ can be determined from concentration dependent grating measurements.

Figure 9 illustrates the results of a calculation of the transient grating observable, $S(t,\tau_r)$, as a function of the probe pulse delay time for various solvent relaxation times.

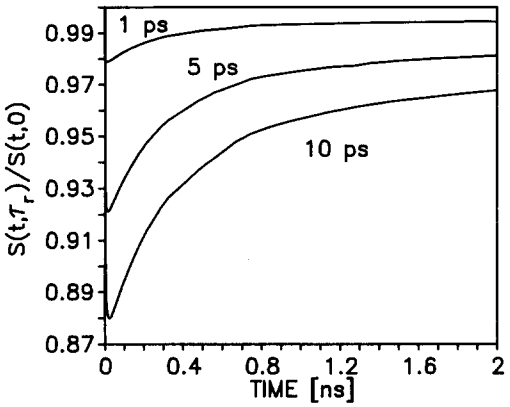

FIG. 9. The transient grating observable as a function of time and τ_r. These curves are all normalized by the transient grating signal when $\tau_r = 0$. $\Delta q = 5kT$, and the other parameters are the same as in Fig. 5.

In these calculations Δq is 5 kT, and the other parameters are given in the figure caption. All curves presented in Fig. 9 are normalized to the transient grating signal with infinitely fast relaxation ($S(t,\tau_r = 0)$). The greatest difference between the transient observable with a finite relaxation time and an infinitely fast relaxation time is found at short time. In Fig. 9 at short time the normalized observable dips well below one showing that $S(t,\tau_r) < S(t,0)$. This is expected because $K_{\text{eff}}(R,t)$ increases with τ_r and thus the ion state would deplete faster with a larger relaxation time. At longer times the normalized observable approaches one because $K_{\text{eff}}(R,t)$ is slowing down to the relaxed value and the ion populations with finite relaxation times and infinitely fast relaxation are steadily approaching the same limiting value.

At long time, $t \gg \tau_r$, the solvent is relaxed and all of the dynamics are due to recombination from ions in the q_∞ state. Fitting the long time data to theory in the long time limit (the theory without solvent relaxation[37] using $K_b(r) = 1/\tau \exp((R_b - R)/a_b)$ for the back transfer rate instead of $K_{\text{eff}}(R,t)$) gives the back transfer parameters a_b, and R_b. Back transfer parameters in the long time limit have been obtained from transient grating experiments.[39] The procedure for extracting the back parameters from long time data has been discussed in detail.[39]

With the forward and back transfer parameters, only three solvent relaxation parameters need to be determined. They are D, the energy diffusion parameter, Δq, the barrier height difference before and after the solvent relaxation, and τ_r, the solvent relaxation constant. As we have shown in Fig. 4, the back transfer rate is not very sensitive to the diffusion parameter D if the relaxation time is short. Solvent relaxation around ions is quite fast so in most experimental situations the D parameter is not important.

The two remaining parameters, Δq and τ_r can be determined in the following way. Obtain the long time parameters using the method discussed in Ref. 39. Calculate curves back to $t = 0$ using the long time parameters. Use this to normalize the short time data in the same way as the calculations in Fig. 9. The function $S(t,\tau_r,\Delta q)/S(t,0)$ should be fit to the resulting curve. The best fit should yield the parameters τ_r and Δq.

IV. CONCLUDING REMARKS

We have developed a theory to describe the role of solvent relaxation in electron back transfer following electron transfer from an optically excited donor to randomly distributed acceptors. The solvent dynamics are included by using a time dependent electron back transfer rate, $K_{\text{eff}}(R,t)$. The solvent relaxation process is parameterized by τ_r, the relaxation time, D, the solvent energy diffusion constant, and Δq the electron back transfer potential barrier height difference between the relaxed and unrelaxed solvent configurations. We also derived an expression for the ensemble averaged donor cation state population probability, $\langle P_{ct}(t) \rangle$, as a function of these solvent parameters.

Solvent relaxation stabilizes the ions relative to the neutrals and reduces the back transfer rates. At very short time, back transfer will occur from an essentially unrelaxed solvent structure. The back transfer activation energy from the unrelaxed solvent state is small thus the back transfer rate is large. As solvent relaxation proceeds, the electron back transfer barrier height increases, and back transfer slows. At times long compared to the solvent relaxation time, the distance dependent back transfer rates become time independent. While a reasonable model was employed for the solvent relaxation, the method permits inclusion of further details, such as multiple solvent relaxation times and distance dependent barrier heights.

The relationship between the solvent relaxation parameters and the experimental observables for a transient grating experiment were discussed. It is now possible to experimentally explore the effects of solvent relaxation on the distance and time dependent flow of electron probability from donors surrounded by randomly distributed acceptors, and to obtain information on the solvent relaxation dynamics.

ACKNOWLEDGMENTS

This work was supported by the Department of Energy, Office of Basic Energy Sciences (DE-FG03-84ER13251). Computing equipment was provided by the National Science Foundation Computing Grant (CHE 88-21737).

[1] T. Guarr and G. McLendon, Coordination Chem. Rev. **68**, 1 (1985).
[2] D. Devault, Q. Rev. Biophys. **13**, 387 (1980).
[3] Z. D. Popovic, G. J. Kovacs, and P. S. Vincett, Chem. Phys. Lett. **116**, 405 (1985).
[4] S. F. Fischer and P. O. Scherer, Chem. Phys. **115**, 151 (1987).
[5] H. Taube, *Electron Transfer Reactions Of Complex Ions In Solutions* (Academic, New York, 1970).
[6] G. R. Fleming, J. L. Martin, and J. Breton, Nature **333**, 190 (1988).
[7] K. Kemnitz, N. Nakashima, and K. Yoshihara, J. Phys. Chem. **92**, 3915 (1988).
[8] R. P. Domingue and M. D. Fayer, J. Chem. Phys. **83**, 2242 (1985).
[9] J. D. Simon and S. Su, J. Chem. Phys. **87**, 7016 (1987).
[10] M. McGuire and G. McLendon, J. Phys. Chem. **90**, 2549 (1986).
[11] D. Huppert, V. Ittah, A. Masad, and E. M. Kosower, Chem. Phys. Lett. **150**, 349 (1988).
[12] R. K. Huddleston and J. R. Miller, J. Phys. Chem. **86**, 200 (1982).
[13] K. Kemnitz, Chem. Phys. Lett. **152**, 305 (1988).
[14] D. N. Beratan, J. Am. Chem. Soc. **108**, 4321 (1986).
[15] P. Siders, R. J. Cave, and R. A. Marcus, J. Chem. Phys. **81**, 5613 (1984).
[16] K. I. Zamaraev, R. F. Khairutdinov, and J. R. Miller, Chem. Phys. Lett. **57**, 311 (1978).

[17] S. Strauch, G. McLendon, M. McGuire, and T. Guarr, J. Phys. Chem. **87**, 3579 (1983).
[18] P. Siders and R. A. Marcus, J. Am. Chem. Soc. **103**, 748 (1981).
[19] N. Mataga, Y. Kanda, and T. Okada, J. Phys. Chem. **90**, 3880 (1986).
[20] P. Chen and E. Danielson, J. Phys. Chem. **92**, 3708 (1988).
[21] R. A. Marcus and N. Sutin, Biochim. Biophys. Acta. **811**, 265 (1985).
[22] B. S. Brunschwig, S. Ehrenson, and N. Sutin, J. Am. Chem. Soc. **106**, 6858 (1984).
[23] E. M. Kosower and D. Huppert, Ann. Rev. Phys. Chem. **37**, 127 (1986).
[24] D. J. Lockhart, R. F. Goldstein, and S. G. Boxer, J. Chem. Phys. **89**, 1408 (1988).
[25] N. R. Kestner, J. Logan, and J. Jortner, J. Phys. Chem. **78**, 2148 (1974).
[26] Y. J. Yan, M. Sparpaglione, and S. Mukamel, J. Phys. Chem. **92**, 4842 (1988).
[27] M. Sparpaglione and S. Mukamel, J. Chem. Phys. **88**, 3263 (1988).
[28] H. McConnell, J. Chem. Phys. **35**, 508 (1961).
[29] B. Bagchi, Ann. Rev. Phys. Chem. **40**, 115 (1989).
[30] M. Maroncelli, J. MacInnis, and G. R. Fleming, Science **243**, 1674 (1989).
[31] P. F. Barbara and W. Jarzeba, Acc. Chem. Res. **21**, 195 (1988).
[32] J. D. Simon, Acc. Chem. Res. **21**, 128 (1988).
[33] H. Sumi and R. A. Marcus, J. Chem. Phys. **84**, 4894 (1986).
[34] I. Rips, J. Klafter, and J. Jortner, J. Chem. Phys. **88**, 3246 (1988).
[35] F. Heisel and J. A. Miehe, Chem. Phys. **128**, 323 (1986).
[36] M. Inokuti and F. Hirayama, J. Chem. Phys. **43**, 1978 (1965).
[37] Y. Lin, R. C. Dorfman, and M. D. Fayer, J. Phys. Chem. **90**, 159 (1989).
[38] R. C. Dorfman, Y. Lin, and M. D. Fayer, J. Phys. Chem. (submitted, 1990).
[39] R. C. Dorfman, Y. Lin, and M. D. Fayer, J. Phys. Chem. **93**, 6388 (1989).
[40] F. Deeg and M. D. Fayer, J. Chem. Phys. **91**, 2269 (1989).
[41] S. Su and J. Simon, J. Chem. Phys. **89**, 908 (1988).
[42] E. W. Castner Jr., M. Marconcelli, and G. R. Fleming, J. Chem. Phys. **86**, 1090 (1987).
[43] H. Risken, *The Fokker-Planck Equation* (Springer, Berlin, 1984).
[44] A. Blumen and J. Manz, J. Chem. Phys. **71**, 4694 (1979).
[45] N. Sutin, in *Supramolecular Photochemistry*, edited by Vincenzo Balzani (D. Reidel, Dordrecht, 1987), pp. 73–86.
[46] K. Nelson, R. Casalegno, R. J. Dwayne Miller, and M. D. Fayer, J. Chem. Phys. **77**, 1144 (1982).